JOURNAL OF GEOPHYSICAL RESEARCH, VOL. 106, NO. D14, PAGES 15,015–15,028, JULY 27, 2001

Cloud water contents and hydrometeor sizes during the FIRE Arctic Clouds Experiment

Matthew D. Shupe,[1] Taneil Uttal,[2] Sergey Y. Matrosov,[3] and A. Shelby Frisch[4]

Abstract. During the year-long Surface Heat Budget of the Arctic Experiment (1997–1998) the NOAA Environmental Technology Laboratory operated a 35-GHz cloud radar and the DOE Atmospheric Radiation Measurement Program operated a suite of radiometers at an ice station frozen into the drifting ice pack of the Arctic Ocean. The NASA/FIRE Arctic Clouds Experiment took place during April–July 1998, with the primary goal of investigating cloud microphysical, geometrical, and radiative properties with aircraft and surface-based measurements. In this paper, retrieval techniques are utilized which combine the radar and radiometer measurements to compute height-dependent water contents and hydrometeor sizes for all-ice and all-liquid clouds. For the spring and early summer period, all-ice cloud retrievals showed a mean particle diameter of about 60 μm and ice water contents up to 0.1 g/m^3, with the maximum sizes and water contents at approximately one fifth of the cloud depth from the cloud base. The all-liquid cloud retrievals had a mean effective particle radius of 7.4 μm, liquid water contents up to 0.7 g/m^3, and a mean droplet concentration of 54 cm^{-3}. Maximum retrieved liquid drop sizes, water contents, and concentrations occurred at three fifths of the cloud depth from the cloud base. As a measure of how representative the FIRE-ACE aircraft flight days were of the April–July months in general, retrieval statistics for flight-day clouds are compared to the mean retrieval statistics. From the retrieval perspective the ice particle sizes and water contents on flight days were ~30% larger than the mean retrieved values for the April–July months. Retrieved liquid cloud parameters during flight days were all about 20% smaller. All-ice and/or all-liquid clouds acceptable for these retrieval techniques were observed about 34% of the time clouds were present; at all other times, mixed-phase clouds precluded the use of these single-phase retrieval techniques.

1. Introduction

The microphysical properties of clouds strongly influence their radiative properties. Factors such as phase, hydrometeor size, and the distribution of water mass in the cloud interplay to determine how each individual cloud will affect radiative heating profiles in the atmosphere [*Curry*, 1986; *Curry and Ebert*, 1992; *Stephens et al*., 1990]. In situ aircraft measurements of cloud microphysics are useful but are limited by relatively small sample volumes, restrictively short flight times, and by the fact that the aircraft itself may modify the cloud with complex airstreams and vortices as it samples. Current satellite technologies infer cloud properties with passive remote sensors, which have inherent limitations on providing vertically resolved information, face issues of subpixel variations [*Rossow et al*., 1993] and have considerable problems in the Arctic associated with detecting clouds over snow-/ice-covered surfaces. The difficulty in measuring cloud characteristics has resulted in a spatially and temporally limited observational database, leading to a poor representation of clouds, and particularly Arctic clouds, in global climate models [*Curry et al*., 1996].

In the last decade a set of interrelated techniques has been developed to determine microphysical properties of clouds by combining measurements from surface-based radars with infrared and/or microwave radiometer measurements. These techniques were applied to year-long radar and radiometer measurements taken from an ice camp deployed in the Arctic ocean in 1997–1998 as part of the Surface Heat Budget of the Arctic (SHEBA) experiment [*Perovich et al*., 1999; T. Uttal et al., (Surface Heat Budget of the Arctic, submitted to *Bulletin of the American Meteorological Society*) 2000]. The analysis period covered by this paper coincides with the 4-month NASA/FIRE Arctic Clouds Experiment (ACE), which was a partner research program primarily focused on aircraft measurements during the spring and early summer of 1998 [*Curry et al*., 2000].

2. Instrumentation

The SHEBA radar is a 35-GHz (Ka band) system that measures radar reflectivity, Doppler velocity, and Doppler spectral width. It is a copy of the systems that were designed and built by the NOAA Environmental Technology Laboratory (ETL) for the DOE Atmospheric Radiation Measurement (ARM) Program [*Moran et al*., 1998], with minor modifications to accommodate the Arctic environment and mounting on a ship. This system was designed to run without full-time operators, in

[1]Science and Technology Corporation, NOAA, Environmental Technology Laboratory, Boulder, Colorado.
[2]NOAA, Environmental Technology Laboratory, Boulder, Colorado.
[3]Cooperative Institute for Research in Environmental Sciences, University of Colorado, NOAA, Environmental Technology Laboratory, Boulder, Colorado.
[4]Cooperative Institute for Research in the Atmosphere, Colorado State University, NOAA, Environmental Technology Laboratory, Boulder, Colorado.

Paper number 2000JD900476.
0148-0227/01/2000JD900476$09.00

remote locations, and with a minimum of maintenance and oversight. The system points vertically and produces long-term and continuous profiles of radar parameters through clouds and light precipitation. The single-polarization system uses a low-peak-power, high-duty-cycle traveling wave tube amplifier (TWTA) transmitter, a high-gain antenna, and pulse compression techniques. The pulse compression techniques make this radar particularly sensitive, with an estimated detection threshold of −47 dBZ at 5 km above ground level (agl). In the Arctic, attenuation of the radar signal is seldom an issue, and comparisons with lidar data indicate that tenuous cirrus clouds below the sensitivity threshold of the radar occur only about 15% of the time (J. M. Intrieri et al., Annual cycle of Arctic cloud geometry and phase from radar and lidar at SHEBA, submitted to *Journal of Geophysical Research*, 2000). Therefore the vertical reflectivity profiles from the SHEBA radar are considered to be a fairly complete description of cloudiness, precipitation, and diamond dust over the ice camp. Reflectivities measured by the radar provide the foundation for both the liquid and the ice water retrievals discussed in section 3.

The Atmospheric Emitted Radiance Interferometer (AERI) [*Revercomb et al*., 1993] measures the downward absolute infrared spectral radiance (in units of watts per square meter per steradian per wavenumber). The spectral range of the AERI channel 1 is 500 cm^{-1} (20 μm) to 3300 cm^{-1} (3 μm), with a spectral resolution of 1.0 cm^{-1}. The instrument field of view is 1.3°, and a calibrated sky radiance spectrum is produced approximately every 7.1 min. For the retrievals presented in this paper, the infrared brightness temperature is calculated from the average radiance over a 25 cm^{-1} band centered on 900 cm^{-1} (11.1 μm). During periods when the AERI was not operational, a Pyrometrics Corporation infrared thermometer (IRT), which measures the radiance between 9.6 and 11.5 μm, was used. The IRT has the disadvantage of a minimum measurable brightness temperature of −60°C, which is often considerably warmer than the Arctic sky.

The microwave radiometer used at SHEBA is a Radiometrics WVR-1100 with receivers at 23.8 and 31.4 GHz. Brightness temperatures measured by the radiometer at these frequencies are used to derive the liquid water path (LWP) and the integrated water vapor amount in ~2-min intervals. Initial discrepancies between the radiometer-derived LWP and the LWP estimates from aircraft in situ measurements have lead to a reprocessing of the radiometer data. More recent data (compared to those used in the original ARM-processing algorithm) on the dielectric constants of supercooled water were incorporated into the retrieval, resulting in LWP values that are in better agreement with the in situ estimates. Uncertainty in the dielectric constants still exists, however, with retrieved LWP varying in different models by as much as 20% at −10°C (E. Westwater, personal communication, 2000). All radiometers discussed here were operated by the ARM program, and data acquisition and calibration were done in accordance with ARM data standards.

3. Retrieval Techniques

There are a variety of radar-radiometer retrieval techniques for inferring cloud microphysics which utilize different combinations of radiances, Doppler velocities, radar reflectivities and radar spectral widths [*Frisch et al*., 1995; *Mace et al*., 1998; *Matrosov*, 1997; *Sassen et al*., 1999]. These techniques have been discussed at length in the literature; the purpose of this section will be to summarize the salient points of the techniques that were utilized in this analysis of the FIRE-ACE experiment data. Liquid retrieval papers by *Frisch et al*. [1998], A. S. Frisch et al. (On the retrieval of effective radius with cloud radars, manuscript in preparation, 2000), and an ice retrieval paper by *Matrosov* [1999] will be cited frequently and will hereinafter be referred to as F98, F00, and M99, respectively.

3.1. Liquid Retrievals

The technique for determining liquid water content from radar reflectivity and integrated liquid water path retrieved from microwave radiometer measurements was first presented by *Frisch et al*. [1995] and developed further by F98, which showed that retrieval of the water profile does not depend on a lognormal droplet distribution assumption and that the method is independent of radar calibration errors. This retrieval is based on the assumption that both the cloud droplet concentration and the width of the particle size distribution are constant with height. Using these assumptions, it is possible to write the relationship between liquid water content (LWC) and radar reflectivity Z as

$$\mathrm{LWC}(h) = \frac{0.52\rho_w}{k} N^{1/2} Z(h)^{1/2}, \tag{1}$$

where h is the height coordinate, ρ_w is the density of water in g/cm^3, k is a constant relating the sixth and third moments of the droplet distribution, N is the constant with height droplet concentration in cm^{-3}, reflectivity is in units of m^3, and LWC is in units of g/m^3. Liquid water path (LWP) can then be written as

$$\mathrm{LWP} = \sum_{h=1}^{M} \mathrm{LWC}_h \Delta h = \frac{0.52\rho_w}{k} N^{1/2} \sum_{h=1}^{M} Z(h)^{1/2} \Delta h, \tag{2}$$

where Δh is the radar's vertical resolution, and the summation is over the total cloud thickness. Solving (2) for $N^{1/2}$ and substituting into (1) yields an equation for LWC in terms of reflectivity and integrated liquid water path:

$$\mathrm{LWC}(h) = \mathrm{LWP} \frac{Z(h)^{1/2}}{\sum_{h=1}^{M} Z(h)^{1/2} \Delta h}, \tag{3}$$

where LWP is retrieved from measurements taken by the microwave radiometer. On the basis of uncertainties in Z and LWP (about 10 and 20%, respectively), the uncertainty in LWC from (3) is about 21%.

The droplet effective radius (R_e) retrieval technique described by F00 is independent of the LWC retrieval; therefore different assumptions regarding particle concentration are applied. This retrieval is based on an empirical relationship between concentration and calculated radar reflectivity that was derived from a set of particle size spectra measured by an airborne Particle Measuring Systems (PMS) Forward Scattering Spectrometer Probe (FSSP-100). To make the F00 technique specific to Arctic clouds, FSSP measurements made during the FIRE ACE from the University of Washington (UW) Convair 580 and the National Center for Atmospheric Research (NCAR) C-130 were used in place of data collected in Oklahoma as described by F00. In situ data for developing this relationship were only considered when the total concentration

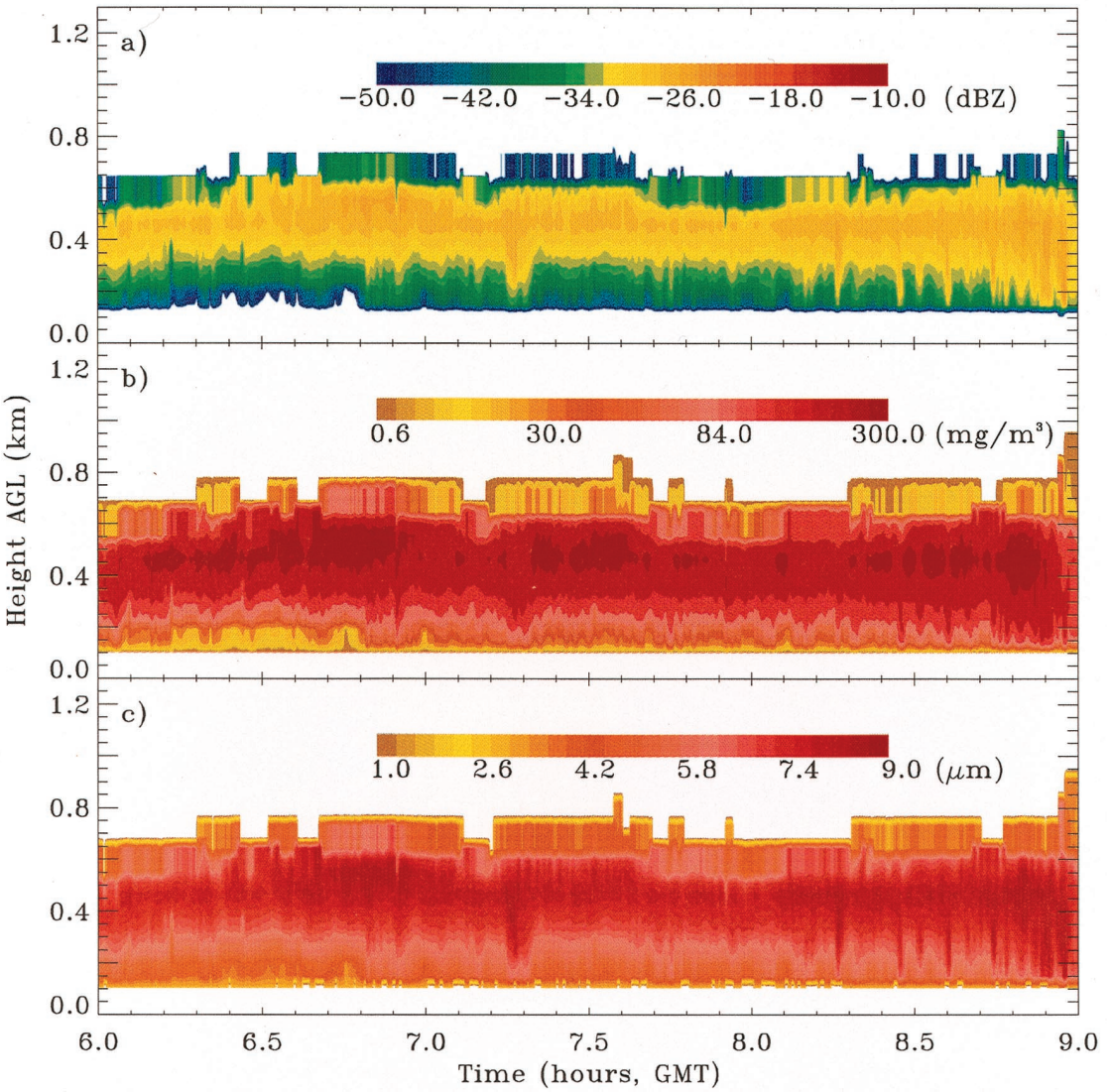

Plate 1. Time-height contours for June 4, 1998, of (a) radar reflectivity, (b) retrieved liquid water content, and (c) retrieved effective particle radius.

of liquid size particles measured by the FSSP was greater than 10 cm^{-3} and the total concentration of particles larger than about 50 μm (measured by a PMS 1D-C on the UW aircraft and a PMS OAP-260X on the NCAR aircraft) was less than 1 L^{-1}. As described by F00, the concentration and reflectivity data were fit to yield a value of N, in 1-dBZ bin widths, which minimized the standard deviation in R_e using the relationship

$$R_e = 0.5 \frac{Z^{1/6}}{N^{1/6}} e^{-0.5\sigma^2}, \quad (4)$$

where σ is the logarithmic spread of the droplet size distribution. On the basis of the FIRE ACE in situ data mentioned above, σ is 0.34 ± 0.09; therefore a value of 0.34 was used for all retrievals discussed here. This value of σ is slightly different from the F00 value of 0.32. The empirical N-dBZ relationship derived via the F00 technique is

$$N(\text{dBZ}) = 122.19 + 3.67(\text{dBZ}) + 0.100(\text{dBZ})^2 + 0.0020(\text{dBZ})^3 + 0.000014(\text{dBZ})^4. \quad (5)$$

The coefficients of this relationship differ from those of the F00 relationship due to the lower concentrations measured during FIRE ACE. The effective radius is calculated from radar reflectivity by substituting (5) into (4).

The relationship (5) was fit to radar reflectivities between −53 and −10 dBZ since there were few FSSP size spectra yielding inferred reflectivities outside these bounds. This range of reflectivities covered most nonprecipitating liquid clouds observed during the April through July time period; however, to allow for a slightly larger range of reflectivities, (5) was extended to cover the interval from −60 to 0 dBZ. These reflectivity limits, when applied to (4) and (5), correspond to similar range limits in concentration (10–120 cm^{-3}) and droplet effective radius (3–21 μm). The standard deviation of (5) from the in situ measurements of N was ~90%. Taking the uncertainties in N, Z, and σ (90, 10, and 26%, respectively) into account, the uncertainty in R_e from (4) is about 17%.

A 3-hour period from 0600 to 0900 UT on June 4, 1998, demonstrates the liquid cloud retrieval products. This time

period consisted of a fairly stable stratus layer with cloud top near 700 m. Radar reflectivity, the key radar measurable for these retrievals, is shown in Plate 1a, retrieved LWC is shown in Plate 1b, and retrieved R_e is shown in Plate 1c. Since estimates of LWP from the microwave radiometer data are not affected by ice layers, the liquid retrievals can be applied to cases when ice and liquid are in the same vertical column but in separate cloud layers, for instance, high level cirrus above a low liquid stratus cloud. In these cases, such as the one described in section 4, the retrieval is performed only through the depth of the low-altitude cloud, which is presumed to contain all of the liquid in the column. The liquid cloud retrieval techniques are also applicable when the liquid is distributed through multiple, all-liquid layers.

3.2. Ice Retrievals

A number of related techniques have been developed to determine ice-cloud water contents and particle sizes. *Matrosov et al*. [1992] used brightness temperatures from an IR radiometer (10–11.4 μm) and radar reflectivities to determine ice water path (IWP) and a layer mean particle size integrated over the cloud depth. The technique was expanded by *Matrosov et al*. [1994] and *Matrosov* [1997] by incorporating vertical Doppler velocities so that profiles of ice water contents and particle sizes could be retrieved, rather than just layer-averaged quantities. During the SHEBA experiment, a combination of small but continuous shifts in the pack ice and hence the pitch of the ship resulted in misalignments of the radar antenna from vertical, which introduced some contamination of the vertical velocities with a component from the horizontal winds. As a result the technique described by *Matrosov* [1997] could not be applied. Therefore a third technique described by M99, based on tuned regressions between reflectivity and cloud parameters, is utilized so that profiles of ice water content and particle characteristic size can be estimated without Doppler information.

Over the years, a number of empirical power-law regressions have been proposed for relating ice water content (IWC) and radar reflectivity [*Atlas et al*., 1995; *Liao and Sassen*, 1994; *Matrosov*, 1997; *Sassen*, 1987; *Sassen and Liao*, 1996] using equations of the form

$$\mathrm{IWC} = aZ^b. \tag{6}$$

A wide range of "a" and "b" coefficients have been obtained, often from aircraft data, for varying cloud conditions and geographical locations. The coefficients have varied enough to cause large differences in resulting IWC values [*Matrosov*, 1997], demonstrating the inaccuracies involved in applying any single regression to data sets that include the diversity of cloud conditions that might be introduced by season, cloud altitude, or air mass characteristics. The "tuned regression" technique described by M99 utilizes (6) but determines unique coefficients on the basis of the observed radar reflectivities and optical thickness inferred from IR radiometer measurements.

Atlas et al. [1995] showed that the exponent "b" in (6) is related to the variability of the characteristic particle size, with higher size variability resulting in a lower value of "b." On the basis of observed vertical distributions of ice particle size variability for which full remote sensing retrievals (as described by *Matrosov* [1997]) were possible, M99 assumes that "b" varies with height, decreasing from about 0.7 near the cloud base to about 0.6 near cloud top.

Tuning the "a" coefficient requires accurate measurement of the IR brightness temperature, which provides information about the cloud IR optical thickness τ of optically thin clouds (i.e., $\tau \leq 3$) [*Matrosov et al*., 1998]. Combining τ and the layer-mean radar reflectivity, Z_m, the ice water path (IWP) can then be inferred [*Matrosov et al*., 1992]. Integration of (6) over the cloud depth, with the assumption that "a" is constant with height, shows the relationship among "a," IWP, and Z to be

$$a = \frac{\mathrm{IWP}(Z_m, \tau)}{\int Z(h)^{b(h)}\, dh}. \tag{7}$$

IWC is then calculated by substituting (7) into (6) and using the height-dependent value of b.

Ice particle characteristic size is calculated as a function of the IWC using the relationship

$$Z = GD_o^3\mathrm{IWC}, \tag{8}$$

where Z is in mm^6/m^3, D_o is in μm, and IWC is in g/m^3. In this relationship the characteristic size, D_o, describing the particle size distribution is the median diameter of the equal-volume sphere, and the coefficient G is a function of the particle shape, density, and size distribution [*Atlas et al*., 1995]. By using a relationship associating particle bulk density to size [*Brown and Francis*, 1995], G can be related to D_o [M99] by

$$G(D_o) \approx 74 \times 10^{-6} D_o^{-1.1}. \tag{9}$$

In (9) an exponential particle size distribution and quasi-spherical particles were assumed on the basis of a preliminary perusal of data from a 2D-C probe on the Canadian Convair 580 aircraft that flew during FIRE ACE. The uncertainties introduced into the retrieval due to these assumptions are discussed by M99. The mean particle diameter can be calculated by substituting (9) into (8):

$$D_{\mathrm{mean}} = 0.28\left(\frac{Z}{74 \times 10^{-6}\mathrm{IWC}}\right)^{1/1.9}. \tag{10}$$

The value of 0.28 is the conversion factor from D_o to mean diameter D_{mean}, assuming an exponential particle size distribution. *Matrosov et al*. [1998] showed relative standard deviations of retrieved D_o and IWC from in situ measurements to be 30 and 55%, respectively, using techniques similar to those described above.

For these ice retrievals, since IWC and "a" are directly related, and size calculations are based on IWC, the accuracy of the technique is highly dependent on good values of "a." There were several circumstances during the FIRE-ACE period which hindered the accurate calculation of "a" on a case-by-case basis, making the full-tuned regression technique applicable ~15% of the time that all-ice clouds were observed. A primary limitation in the determination of "a" was the AERI being inoperable for a significant fraction of the time during the months of May, June, and July. Although in some instances measurements from the IRT could be substituted, frequently the sky brightness temperature was below the −60°C IRT detection threshold. It was also common for an upper level ice cloud to be radiometrically obscured by low-level liquid clouds. Finally, it was sometimes the case that clouds were so optically thin that the uncertainty in determining "a" by the tuned regression technique became large, and the accuracy of the retrieval was in question.

In cases where ice clouds were too optically thin for the

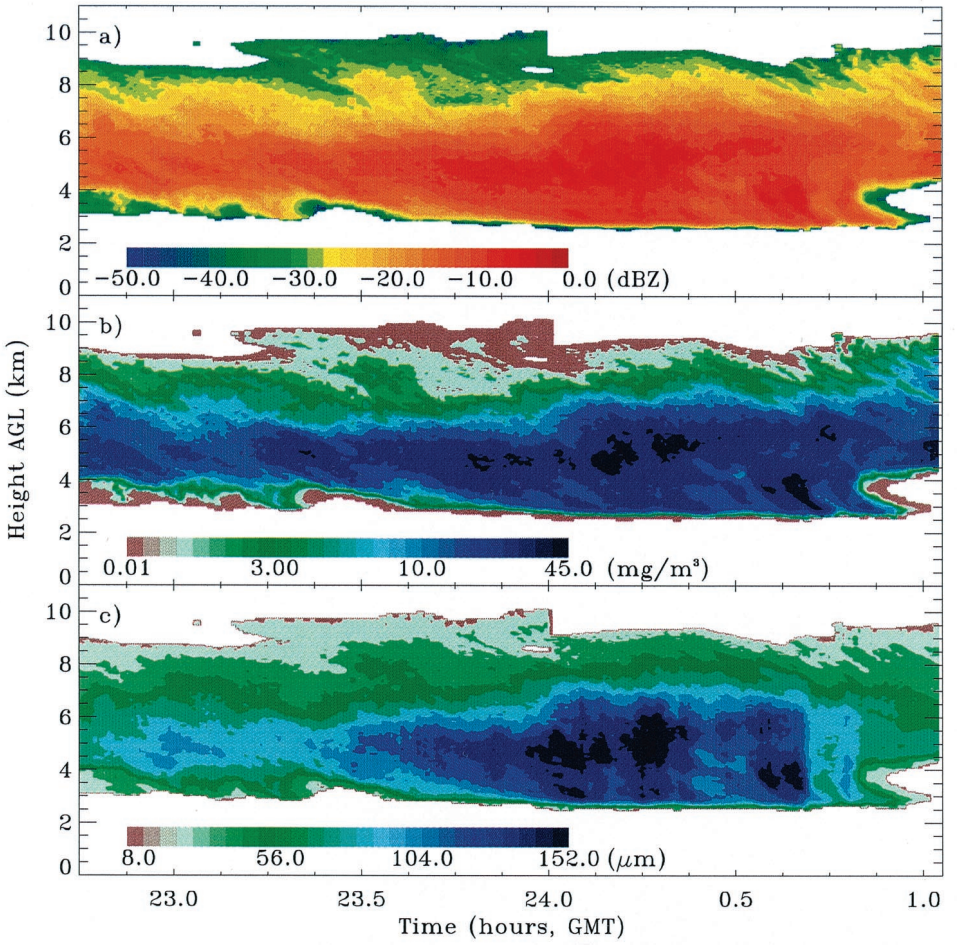

Plate 2. Time-height contours for May 26–27, 1998, of (a) radar reflectivity, (b) retrieved ice water content, and (c) retrieved mean particle diameter.

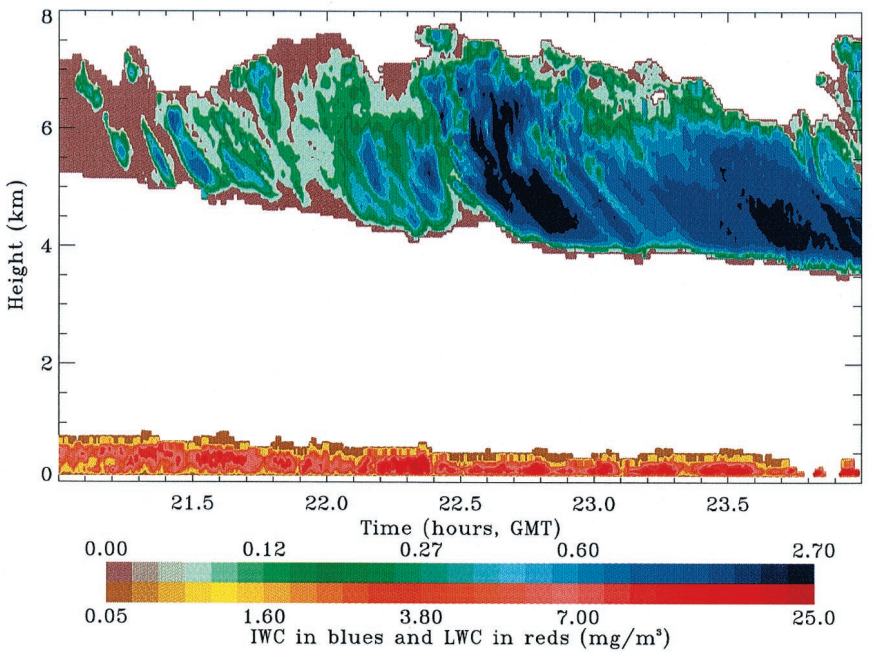

Plate 3. Time-height contours for June 10, 1998, of ice (blue) and liquid (red) water contents.

Table 1. Cloud-Type Characterization, in Percent of Time, for FIRE-ACE Months

	Fractional Cloudiness	All Liquid (One Layer)	All Ice (One Layer)
April	93.1	4.2 (0.0)	21.3 (7.0)
May	88.0	23.2 (3.8)	17.6 (6.1)
June	87.8	18.4 (4.5)	23.4 (7.9)
July	93.9	23.2 (5.6)	15.0 (5.9)
Total	90.7	17.3 (3.5)	19.3 (6.7)

Fractional cloudiness is the total percentage of time clouds observed by the radar. All other values are percentages of when clouds were present (i.e., portions of the fractional cloudiness). Single-phase cloud percentages are shown for both liquid and ice clouds. Single-phase and single-layer cloud percentages are shown in parentheses.

tuned regression technique, no retrievals were performed. However, to expand the retrieval analysis to the ice clouds with the other limiting physical circumstances, (6) was applied with an assigned value of "*a*" and the same assumed form of "*b*." If reasonable calculations of "*a*" using the tuned regression were possible for any part of a cloud, these values were extended to cover the full cloud. For cases in which no values of "*a*" could be calculated throughout an entire cloud, the mean "*a*" for the 4-month period was assigned. This type of assignment leads to a larger uncertainty than the tuned regression approach, yet it is significantly better than any a priori coefficient derived from clouds in non-Arctic locations. The mean "*a*" calculated for FIRE ACE was 0.095 ± 0.067 leading to uncertainties of about 70% in IWC and 37% in D_{mean} for this type of ice cloud retrieval.

An ice cloud occurring over the 2-hour period from ~2300 UT on May 26 to 0100 on May 27, 1998, demonstrates the ice retrieval products. This cloud was geometrically thick, but optically thin, with a base at 3 km agl and a top near 10 km agl. Radar reflectivity is shown in Plate 2a, retrieved IWC is shown in Plate 2b, and retrieved D_{mean} is shown in Plate 2c.

4. Results

The cloud radar data set for the SHEBA experiment spanned nearly 1 year, from October 20, 1997 to October 1, 1998. This paper, however, presents statistics of cloud properties for the April–July 1998 time period, which brackets the aircraft flights conducted during the FIRE-ACE program. Within these 4 months, retrievals of water contents, particle characteristic sizes, and particle concentrations were calculated for clouds that appeared to be single phase, either all ice or all liquid. In cases where multiple cloud layers existed, retrievals were also performed if the liquid and ice appeared to be divided into distinct layers. An example of simultaneous all-liquid and all-ice clouds occurred on June 10 (Plate 3). The liquid retrieval was applied through the depth of the low-level stratus, and (6) was applied to the upper level ice cloud using an "*a*" coefficient of 0.095.

Phase determination was made on a case-by-case basis by examining microwave radiometer-derived LWPs, IR brightness temperatures, the structure of the radar reflectivities and Doppler velocities, lidar depolarization ratios, and temperature and humidity profiles from radiosondes. The clouds that were deemed to be single phase generally consisted of low stratus (liquid) and midlevel to upper level cirrus (ice) clouds. The total monthly cloud fraction and the percent of observed clouds that were all liquid or all ice are shown in Table 1. The single-phase criteria were fit ~34% of the time that clouds were observed for the 4-month period, with all-liquid clouds occurring 17% of the time and all-ice clouds occurring 19% of the time. Note that some of the time all-liquid and all-ice clouds occurred simultaneously (<3%). There were no significant trends in the percentages of single-phase clouds over the 4-month period, with the exception that April had a substantially smaller percentage of all-liquid clouds. Also shown in Table 1 (in parentheses) are the subset of clouds that were determined to be single layered as well as single phased and having a cloud base above the lowest radar range gate of 105 m.

In this section, two basic types of cloud microphysical statistics are shown. The first type is the distribution of retrieved parameter values irrespective of height. For the sake of comparing multiple distributions, each has been normalized. The second type of result is the profile of retrieved parameters. Each retrieved profile has been normalized in cloud depth and in magnitude of the retrieved microphysical parameter, therefore mean profiles will have a maximum somewhat less than unity. To demonstrate how representative the FIRE-ACE aircraft flight days were of the entire April–July time period, retrieved parameter distributions and profiles are also shown for clouds observed on flight days although not necessarily sampled by the aircraft. These data are not to be confused with the aircraft in situ measurements, which are not shown in this paper.

4.1. Liquid Cloud Statistics

The normalized frequency distribution of retrieved droplet effective radii for all clouds determined to be liquid during the April–July 1998 time period is illustrated in Figure 1. The distribution shows a broad peak at 7 μm, the minimum calculated R_e is 3 μm, and the maximum is around 20 μm. The mean retrieved value of R_e is 7.4 μm, while the median value of R_e is 6.9 μm. The median value presented here, and in the following sections, is the standard statistical median. These retrieved droplet sizes are similar to liquid cloud in situ measurements made during the 1980 Arctic Stratus Experiment (ASE) [*Curry et al*., 1996], ranging from 3.6 to 11.4 μm with a mean of 7.5 μm and measurements made during the 1995 Arctic Radiation Measurements in Column Atmosphere-Surface System (ARMCAS) Experiment [*Hobbs and Rangno*, 1998], showing average profile R_e ranging from 3 to 12 μm. For comparison purposes, Figure 1 also shows the distribution of retrieved drop sizes for the 7 days on which there were aircraft flights over the ice camp and all-liquid cloud layers were identified. With the exception of May 18 and July 29, most flight-day cases show distributions that have slightly smaller droplet size modes than those of the April–July mean statistics. The mode of the R_e distribution for the seven cases combined is near 5.5 μm, the mean is 6.2 μm, and the range of sizes is generally between 3 and 13 μm.

Normalized frequency distributions of retrieved LWC for the liquid clouds which occurred during the April–July period are shown in Figure 2. The retrieved liquid water contents range from near zero to 0.7 g/m^3 with a mean value of 0.1 g/m^3 and a median value of 0.06 g/m^3. Measurements made during ASE showed a maximum measured LWC of 0.5 g/m^3, while those made during ARMCAS were as high as 0.66 g/m^3 in all-liquid clouds. Again, for comparison purposes, the frequency distributions of retrieved LWC for the all-liquid clouds on seven aircraft flight days are also included. In general, the

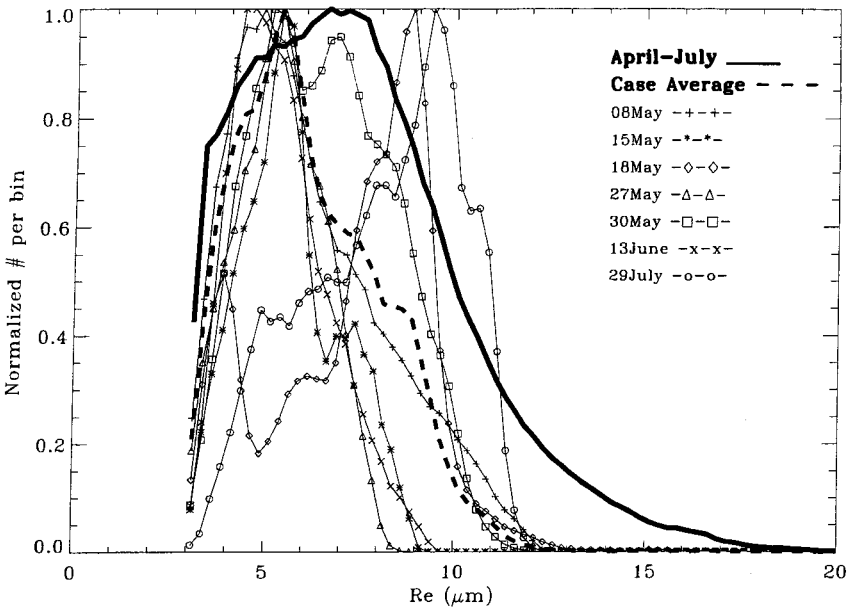

Figure 1. Normalized, retrieved effective radius distributions for the full April–July period (solid line) with retrieved distributions for seven flight-day liquid-cloud cases (symbols w/lines) and the combined flight-cases average (dashed line).

flight-day cases have distributions that are characterized by a more pronounced occurrence of LWC values in the 0.02–0.07 g/m^3 range. The mean LWC for the seven flight-day cases is 0.08 g/m^3, which is 20% smaller than the mean for the entire April–July period.

The April–July normalized distribution of retrieved liquid droplet concentrations (Figure 3) shows values ranging from 10 to 120 cm^{-3} with the lower limit of 10 cm^{-3} an artifact of the −60 dBZ limit in (5). The mean retrieved liquid droplet concentration is 54 cm^{-3}, and the median value is 56 cm^{-3}. Measurements made during ARMCAS showed droplet concentrations that were often below 100 cm^{-3}. The distributions of retrieved concentrations for the seven flight-day cases are quite varied; however, the mean distribution of these cases is similar to the April–July mean distribution, with a mean concentration of 47 cm^{-3}. The slightly smaller retrieved concentrations for flight-day cases are consistent with smaller retrieved water contents and droplet sizes.

For the subset of data considered to be single layer as well as all liquid (see Table 1), droplet size profiles, normalized by cloud depth and maximum droplet size, were calculated (Figure 4a). Many of the liquid clouds observed during the April–

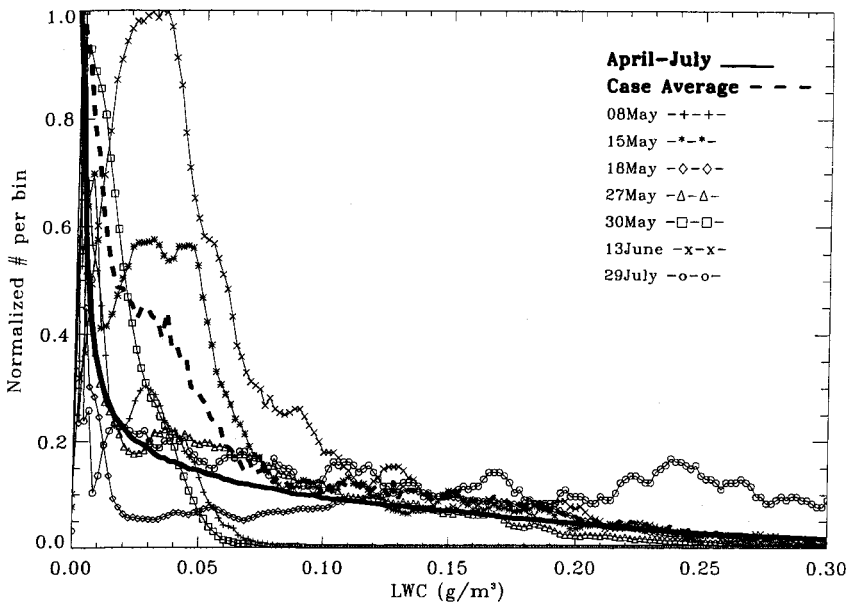

Figure 2. Normalized, retrieved liquid water content distributions for the full April–July period (solid line) with retrieved distributions for seven flight-day liquid-cloud cases (symbols w/lines) and the combined flight-cases average (dashed line).

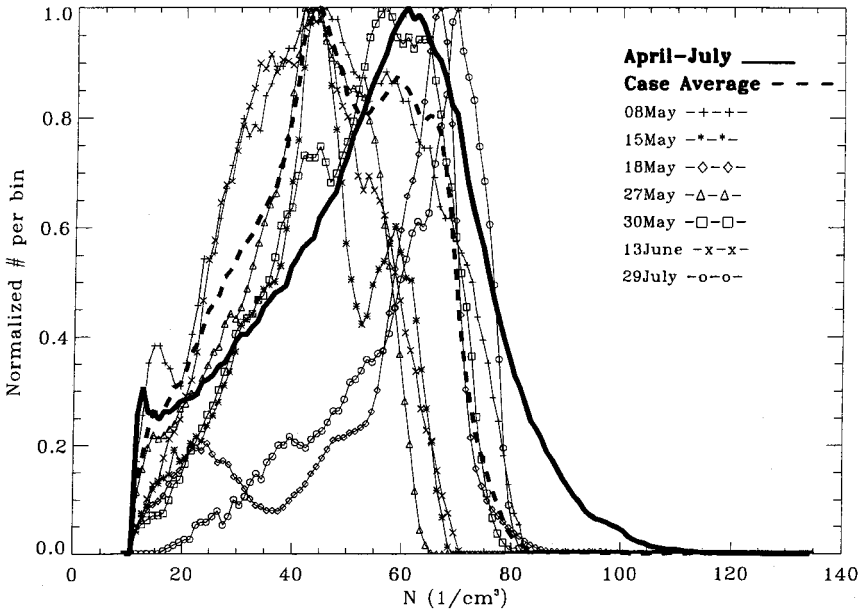

Figure 3. Normalized, retrieved liquid droplet concentration distributions for the full April–July period (solid line) with retrieved distributions for seven flight-day liquid-cloud cases (symbols w/lines) and the combined flight-cases average (dashed line).

July months had bases below the lowest radar range gate (105 m) and were therefore not useful for these profile statistics. The April–July mean profile indicates that on average the largest particles were found at about three fifths of the cloud geometrical depth from the cloud base. Both above and below this level the particle sizes decreased rapidly, with the smallest particles at cloud base. The decrease in particle sizes toward the top of the cloud suggests an evaporation process occurring at cloud top. In general, the retrieved particle size profiles for the individual flight-day cases deemed to be all liquid are within one standard deviation of the mean April–July profile. The general profile shape shows reasonable agreement with the particle size profiles from ASE, as well as with the particle size profiles calculated by *Frisch et al*. [1995] for liquid water stratus clouds measured during the 1992 Atlantic Stratocumulus Transition Experiment (ASTEX). The profile of standard

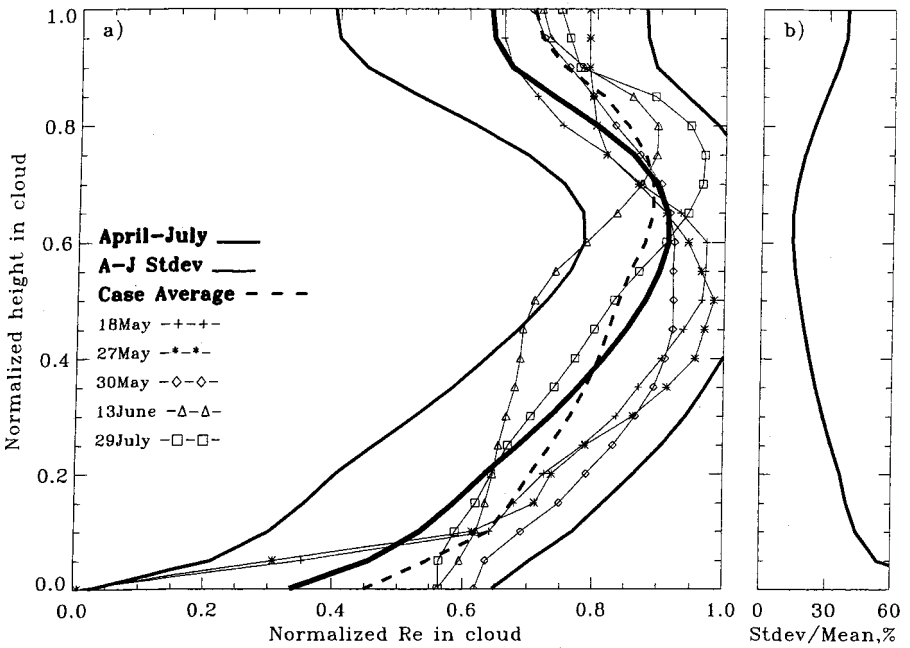

Figure 4. (a) Normalized, retrieved effective radius profiles for April–July (thick line), the April–July mean plus and minus the standard deviation (thin lines), five retrieved liquid-cloud flight cases (symbols w/lines), and the average profile for the five flight-day cases (dashed line). (b) The April–July standard deviation divided by the mean profile, in percent, describing the profile variability.

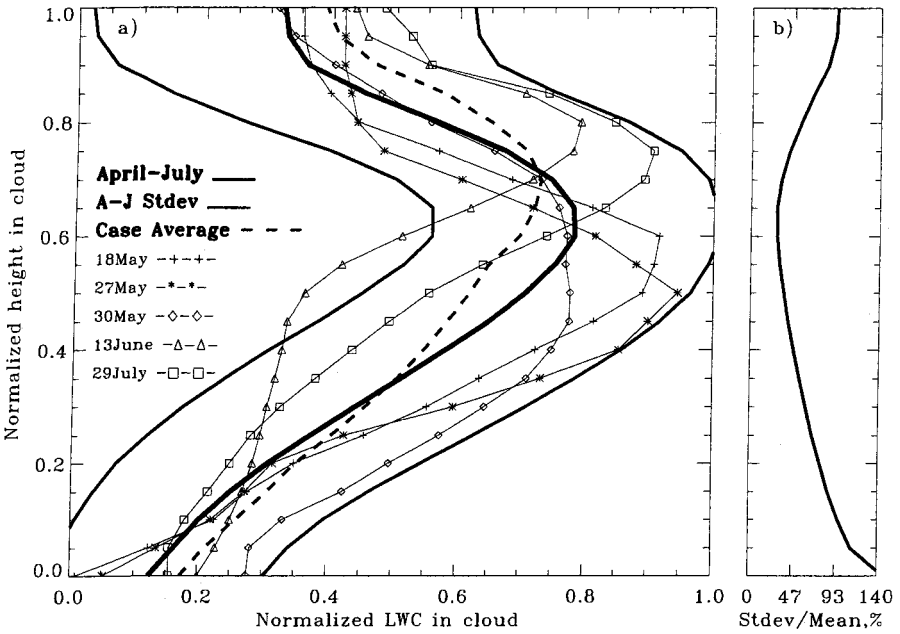

Figure 5. (a) Normalized, retrieved liquid water content profiles for April–July (thick line), the April–July mean plus and minus the standard deviation (thin lines), five retrieved liquid-cloud flight cases (symbols w/lines), and the average profile for the five flight-day cases (dashed line). (b) The April–July standard deviation divided by the mean profile, in percent, describing the profile variability.

deviation divided by mean (in percent), for the April–July period, which provides an estimate of the height-dependent variability from the mean, is shown in Figure 4b. The variability is generally less than 25% in the middle of the cloud, demonstrating consistency in the vertical distribution of liquid particle sizes when normalized in this manner.

Mean, normalized profiles of retrieved LWC for the single-layer, all-liquid clouds occurring in the April–July period and during the seven individual flight-day cases are presented in Figure 5a. As would be expected for a fixed concentration with height, the shape of the LWC profiles is similar to that of the particle size profiles with the largest water contents at three fifths of the cloud depth up from the cloud base. The variability of LWC (Figure 5b) is significantly larger (30–140%) than the variability of R_e (15–60%) due to the fact that LWC values range over 3 orders of magnitude, while R_e only varies over 1 order of magnitude.

The mean, normalized profiles of retrieved liquid droplet concentration (Figure 6) have shapes similar to those of droplet size and water content. Again, the flight-day cases show mean retrieved profiles that are, in general, quite comparable with the mean April–July profile. The variability of the particle concentration profiles ranges from about 20% in the middle of the cloud to about 80% at the cloud base.

4.2. Ice Cloud Statistics

The normalized frequency distribution of retrieved ice particle mean diameters for the clouds determined to be all ice during the April–July time period is shown in Figure 7. The distribution has a single peak at 30 μm, with D_{mean} ranging in size from 7 to 300 μm, a mean retrieved D_{mean} of 60 μm, and a median value of 46 μm. A review of in situ cirrus measurements generally from lower latitudes [*Dowling and Radke*, 1990] discusses "reasonable" ice particle mean diameters of 40–70 μm which bracket the mean retrieved FIRE-ACE value (*Dowling and Radke* [1990] published actual crystal lengths that were converted to mean diameter using equations presented by *Matrosov et al.* [1995] and a range of expected aspect ratios). For comparison purposes the frequency distributions of retrieved D_{mean} for six all-ice flight-day cases are also shown. For the flight-day cases the distributions tend toward larger particle sizes; the distribution for the six cases combined has a peak at 40 μm and a mean value of 75 μm, both of which are about 25% larger than the April–July values.

The normalized frequency distribution of retrieved IWC for the clouds determined to be all ice during the April–July period is presented in Figure 8. Retrieved ice water contents range from near 0 to 0.1 g/m^3 with a mean value of 0.005 g/m^3 and a median value of 0.001 g/m^3. Preliminary comparisons between these ice retrievals and the in situ measurements made by the Canadian Convair 580 on April 28/29 at FIRE ACE show uncertainty estimates (about 30% for D_{mean} and 60% for IWC) similar to those discussed by *Matrosov et al.* [1998]. The individual flight-day-retrieved IWC distributions have shapes similar to the April–July distribution with the April 28 case being a slight exception, showing a larger portion of values at about 0.003 g/m^3. The mean value of retrieved IWC for the six flight-day cases is 0.007 g/m^3, which is 40% larger than the April–July mean and is in agreement with the larger than average particle sizes retrieved during the aircraft flight times.

Normalized profiles of retrieved mean particle diameter were calculated for the single-layer, all-ice clouds (Figure 9a) in the same manner as described for the liquid cloud retrievals. The average April–July profile shows the largest particles at one fifth of the cloud depth from the cloud base, with a steady

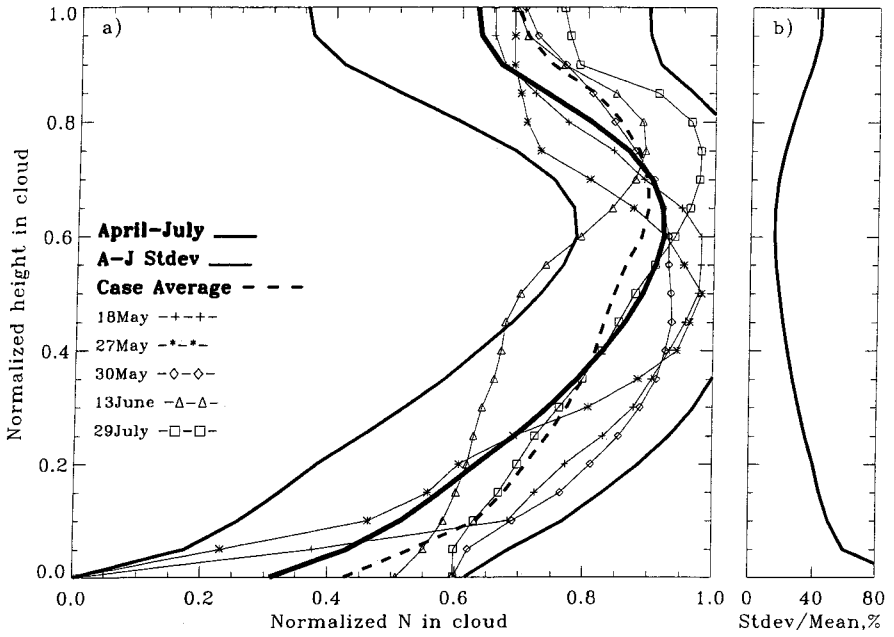

Figure 6. (a) Normalized, retrieved liquid particle concentration profiles for April–July (thick line), the April–July mean plus and minus the standard deviation (thin lines), five retrieved liquid-cloud flight cases (symbols w/lines), and the average profile for the five flight-day cases (dashed line). (b) The April–July standard deviation divided by the mean profile, in percent, describing the profile variability.

particle growth from the top down to this level, and rapid sublimation below this level to the cloud base. All five of the individual flight-day mean retrieved profiles are similar in shape to the April–July profile and, generally, remain within one standard deviation of the 4-month average. The vertical distributions of ice particle size observed here are similar in shape to the vertical distributions presented by *Matrosov* [1997] for ice clouds measured in Kansas, the Madeira Islands, and Arizona. The height-dependent variability is generally smaller than 30% (Figure 9b), demonstrating consistency in the vertical distribution of retrieved particle sizes.

The corresponding, normalized IWC profiles for single-layer, all-ice clouds are shown in Figure 10. As with liquid clouds, the vertical distributions of retrieved water content and particle size in ice clouds have similar shapes, demonstrating the direct relationship between these two parameters. The height-dependent variability of retrieved IWC values is much larger than that of mean particle diameter, again because IWC

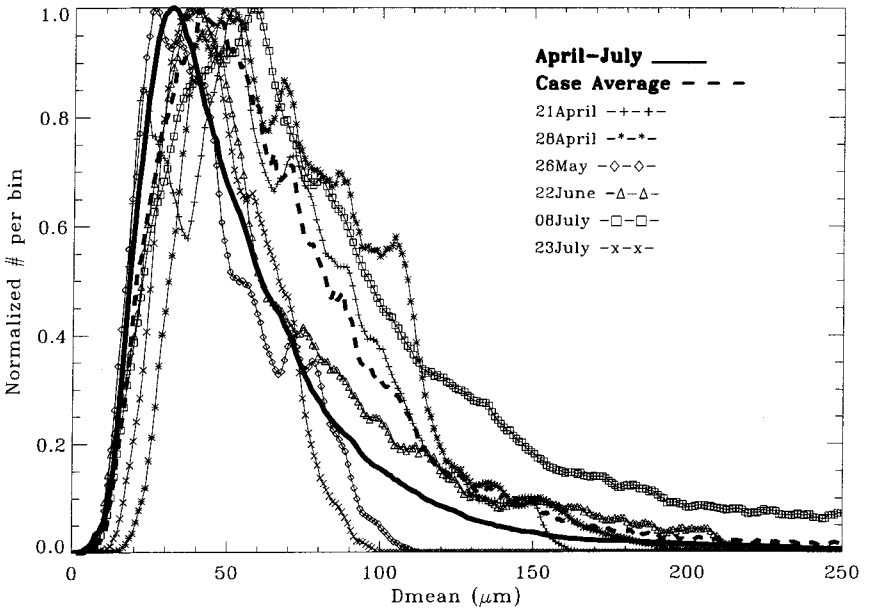

Figure 7. Normalized, retrieved mean particle diameter distributions for the full April–July period (solid line) with retrieved distributions for six flight-day ice-cloud cases (symbols w/lines) and the combined flight-cases average (dashed line).

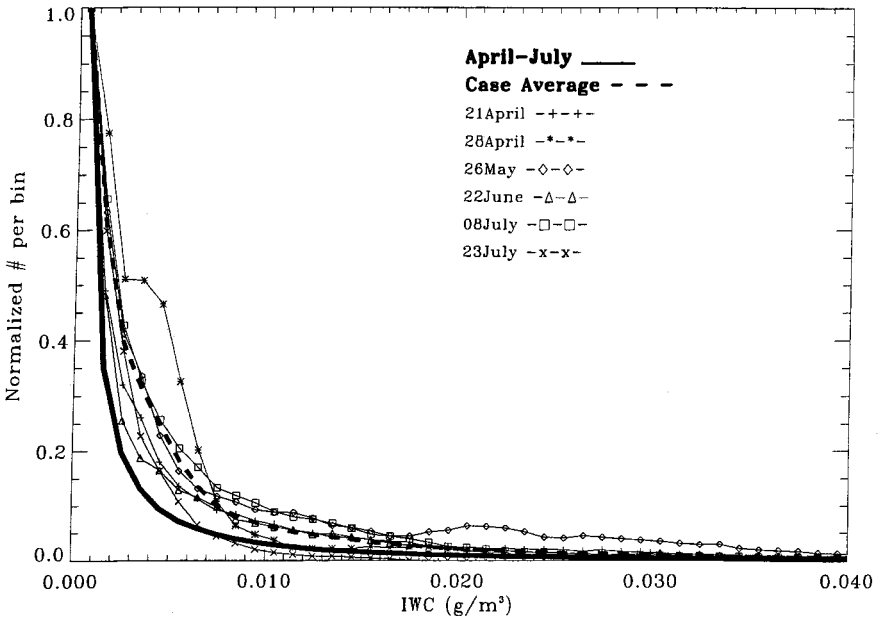

Figure 8. Normalized, retrieved ice water content distributions for the full April–July period (solid line) with retrieved distributions for six flight-day ice-cloud cases (symbols w/lines) and the combined flight-cases average (dashed line).

values range over 4 orders of magnitude, while mean diameters generally range over 2 orders of magnitude.

5. Summary and Future Work

A suite of remote-sensing, cloud microphysics retrieval techniques was applied to ground-based radar and radiometer measurements made during the months of April–July 1998 as part of the FIRE-ACE and SHEBA programs. The techniques, which are summarized in this paper, were applied to all clouds determined to be of a single phase, i.e., all ice or all liquid. The application of these techniques has led to the compilation of a large and unique set of retrieved microphysical data for the Arctic Ocean region. Retrieved parameter ranges, means, and medians covering the full 4-month FIRE-ACE period

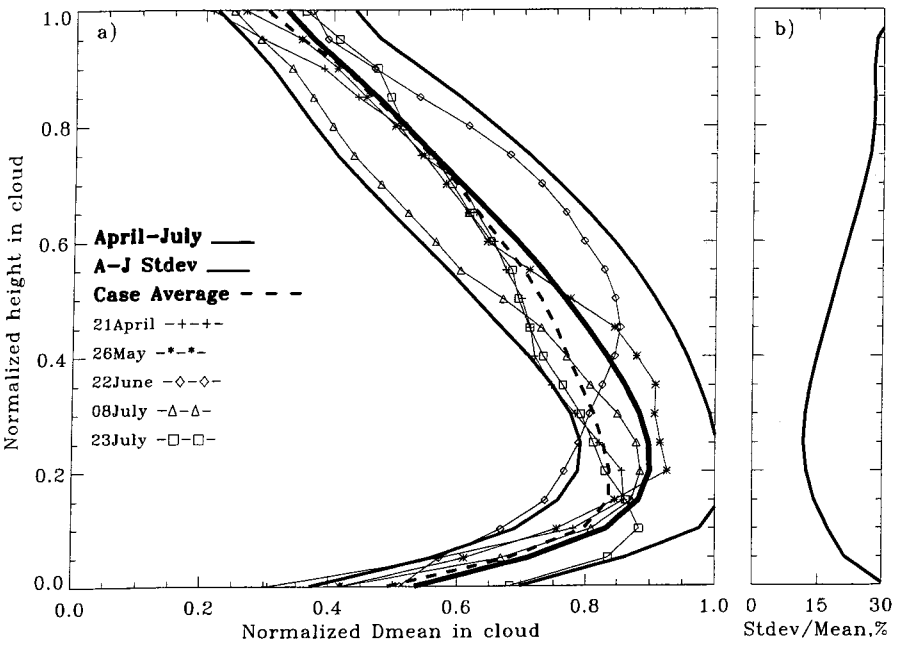

Figure 9. (a) Normalized, retrieved mean particle diameter profiles for April–July (thick line), the April–July mean plus and minus the standard deviation (thin lines), five retrieved ice-cloud flight cases (symbols w/lines), and the average profile for the five flight-day cases (dashed line). (b) The April–July standard deviation divided by mean profile, in percent, describing the profile variability.

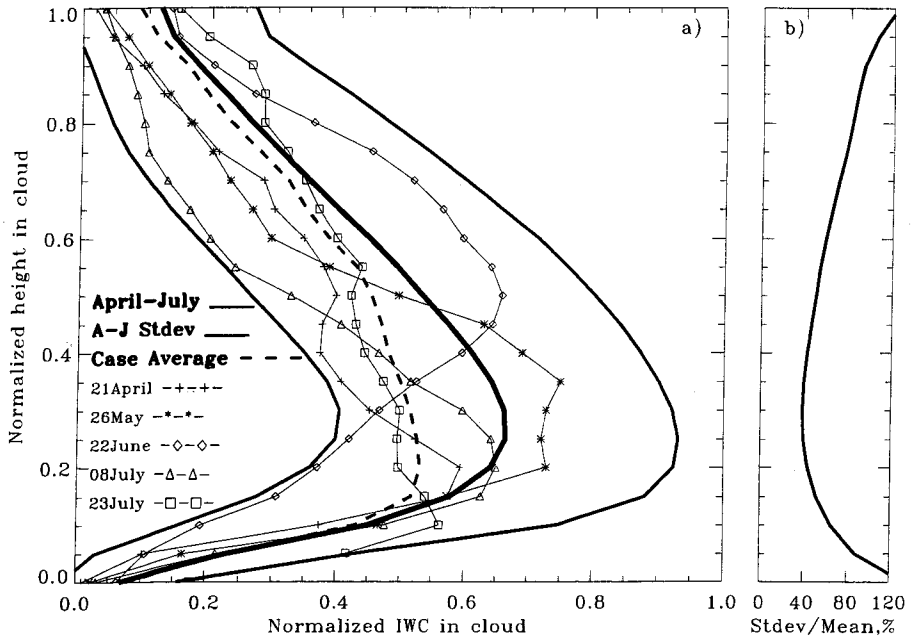

Figure 10. (a) Normalized, retrieved ice water content profiles for April–July (thick line), the April–July mean plus and minus the standard deviation (thin lines), five retrieved ice-cloud flight cases (symbols w/lines), and the average profile for the five flight-day cases (dashed line). (b) The April–July standard deviation divided by mean profile, in percent, describing the profile variability.

are summarized in Table 2. Uncertainties for each of these parameters and the employed retrieval techniques are summarized in Table 3.

Generally, the retrieved liquid-cloud parameter values are similar in magnitude and vertical distribution to previous in situ measurements made in the Arctic [*Curry et al*., 1996; *Hobbs and Rangno*, 1998]. Liquid-cloud droplet size, water content, and concentration increase from the cloud base to about three fifths of the cloud geometrical depth from the base, then decrease up to the cloud top. The shape of these retrieved profiles is in reasonable agreement with stratus cloud profiles presented in the literature [*Curry*, 1986; *Frisch et al*., 1995], and the relatively low variability of these profiles show consistency over the full 4-month period. The retrieved values of liquid water content are linearly related to the microwave radiometer-derived liquid water path, which because of differing models for the dielectric constants of water has an uncertainty of 15–25% for supercooled liquid clouds.

Retrieved ice cloud particle sizes and water contents show reasonable agreement in preliminary comparisons with in situ measurements made at FIRE ACE. Normalized profiles of these retrieved microphysical parameters demonstrate that ice cloud mean particle diameters and ice water contents increase sharply from cloud base to one fifth of the cloud geometrical depth from the base and then decrease up to the cloud top. This profile shape is similar to the vertical profiles presented by *Matrosov* [1997] for lower latitude clouds. In the future, more in-depth case study comparisons, both for all-ice and all-liquid clouds, will be made between the retrieved parameters presented here and the in situ measurements made during FIRE ACE.

This study also assesses how representative the single-phase clouds on individual FIRE-ACE flight days were of the April–July time period in general. These results are summarized in Table 4. Generally, the all-liquid clouds occurring on flight

Table 2. Range, Mean, and Median for Each Retrieved Parameter

Parameter	Range	Mean	Median
R_e, μm (liquid)	3–20	7.4	6.9
LWC, g/m^3 (liquid)	0–0.7	0.1	0.06
N, cm^{-3} (liquid)	10–120	54	56
D_{mean}, μm (ice)	7–300	60	46
IWC, g/m^3 (ice)	0–0.1	0.005	0.001

Retrieved ranges are based on 99.9% of the data in order to remove extreme outliers.

Table 3. Uncertainties in Retrieved Parameters

Retrieved Parameter	Uncertainty
LWC (liquid)[b]	21%
R_e (liquid)[b]	17%
N (liquid)[a]	90%
D_{mean} (ice)[a] (tuned regression)	30%
D_{mean} (ice)[b] (empirical regression)	37%
IWC (ice)[a] (tuned regression)	60%
IWC (ice)[b] (empirical regression)	70%

Note that two ice retrieval techniques are described.
[a]Uncertainty based on comparison with in situ aircraft data.
[b]Uncertainty based on standard error propagation analysis.

Table 4. Mean Retrieved Microphysical Parameters for the Full April–July Time Period and for Flight-Day Cases During Those Months (Including the Percentage Difference of the Flight-Day Case Mean From the April to July Mean)

Parameter	April–July Mean	Flight-Day Case Means	Percent Different
R_e, μm (liquid)	7.4	6.2	16%
LWC, g/m^3 (liquid)	0.1	0.08	20%
N, cm^{-3} (liquid)	54	47	13%
D_{mean}, μm (ice)	60	75	25%
IWC, g/m^3 (ice)	0.005	0.007	40%

days showed smaller retrieved droplet effective radii, liquid water contents, and concentrations than the April–July mean values by about 16, 20, and 13%, respectively. The opposite was observed for the flight days containing all-ice clouds. Flight-day-retrieved ice particle mean diameters were about 25% larger than the April–July mean value, and ice water contents were 40% larger. Vertical distributions of all ice and liquid parameters through the cloud depth show that the flight-day retrieval cases were generally within one standard deviation of the April–July mean retrieved profiles. Aircraft flight data should be interpreted in view of the fact that *Minnis et al*. [this issue] have shown diurnal variations in cloud properties, and all aircraft flights took place between ~2000 and 0100 UT.

The single-phase condition limited the retrieval techniques presented here to about 34% of the time clouds occurred during the April–July period. Application of these retrieval techniques, or hybridizations thereof, to mixed-phase clouds will likely be less successful [*Hobbs et al*., this issue]. New techniques are, however, being developed which may allow for the retrieval of ice parameters in mixed-phase clouds by using only radar reflectivity and Doppler velocity measurements. All of the retrieval techniques presented here will be applied to the full SHEBA year of radar and radiometer data in future analyses.

Acknowledgments. This work was supported by the NASA FIRE-ACE program under contract L64205D, the NSF SHEBA program under agreement OPP-9701730, and the NASA EOS Validation Program under contract S-97895-F. We would like to thank the program managers Bob Curran, Michael Ledbetter, and David O'C Starr. Contributions by S. Frisch were supported by interagency agreement DE-A103-97ER62342/A002 with the U.S. Department of Energy (DOE). Microwave and IR radiometer data were obtained from the Atmospheric Radiation Measurement Program sponsored by the DOE. Aircraft data were obtained from the University of Washington Cloud and Aerosol Research Group (CARG) Convair 580 research aircraft under the scientific direction of Peter Hobbs, and the NCAR Research Aviation Facility C-130 research aircraft. The CARG participation in this study was supported by NSF grant OPP-9808163 and NASA grants NAG-1-2079 and NCC5-326. Radiosonde data were obtained from the SHEBA Project Office at the University of Washington, Applied Physics Laboratory (UW/APL). Duane Hazen and Wendi Madsen of NOAA/ETL provided the engineering and programming expertise for the cloud radar. The logistics of deployment at the SHEBA site was greatly aided by the efforts of Kevin Widener and Bernie Zak of the DOE/ARM Program. We would like to thank ETL scientists Jeffrey Otten, Janet Intrieri, and Ann Keane who spent many weeks at the SHEBA ice camp monitoring radar operations. Finally, the collection of these valuable, year-long data sets would not have been possible without the support of the SHEBA logistics team from UW/APL and the crew of the Canadian Coast Guard Ship *Des Grosseilliers*.

References

Atlas, D., S. Y. Matrosov, A. J. Heymsfield, M.-D. Chou, and D. B. Wolff, Radar and radiation properties of ice clouds, *J. Appl. Meteorol*., *34*, 2329–2345, 1995.

Brown, P. R. A., and P. N. Francis, Improved measurements of the ice water content in cirrus using a total-water probe, *J. Atmos. Oceanic Technol*., *12*, 410–414, 1995.

Curry, J. A., Interactions among turbulence, radiation and microphysics in Arctic stratus clouds, *J. Atmos. Sci*., *43*, 90–106, 1986.

Curry, J. A., and E. E. Ebert, Annual cycle of radiation fluxes over the Arctic Ocean: Sensitivity to cloud optical properties, *J. Clim*., *5*, 1267–1280, 1992.

Curry, J. A., W. B. Rossow, D. Randall, J. L. Schramm, Overview of Arctic cloud and radiation characteristics, *Bull. Am. Meteorol. Soc*., *9*, 1721–1764, 1996.

Curry, J. A., et al., FIRE Arctic Clouds Experiment, *Bull. Am. Meteorol. Soc*., *81*, 5–29, 2000.

Dowling, D. R., and L. R. Radke, A summary of the physical properties of cirrus clouds, *J. Appl. Meteorol*., *29*, 970–978, 1990.

Frisch, A. S., C. W. Fairall, and J. B. Snider, Measurements of stratus cloud and drizzle parameters in ASTEX with a Ka-band Doppler radar and microwave radiometer, *J. Atmos. Sci*., *52*, 2788–2799, 1995.

Frisch, A. S., G. Feingold, C. W. Fairall, T. Uttal, and J. B. Snider, On cloud radar and microwave radiometer measurements of stratus cloud liquid water profiles, *J. Geophys. Res*., *103*, 23,195–23,197, 1998.

Hobbs, P. V., and A. L. Rangno, Microstructures of low and middle-level clouds over the Beaufort Sea, *Q. J. R. Meteorol. Soc*., *124*, 2035–2071, 1998.

Hobbs, P. V., A. L. Rangno, M. D. Shupe, and T. Uttal, Airborne studies of cloud structures over the Arctic Ocean and comparisons with retrievals from ship-based remote sensing measurements, *J. Geophys. Res*., this issue.

Liao, L., and K. Sassen, Investigation of relationships between Ka-band radar reflectivity and ice and liquid water content, *Atmos. Res*., *34*, 231–248, 1994.

Mace, G. G., T. P. Ackerman, P. Minnis, and D. F. Young, Cirrus layer microphysical properties derived from surface-based millimeter radar and infrared interferometer data, *J. Geophys. Res*., *103*, 23,207–23,216, 1998.

Matrosov, S. Y., Variability of microphysical parameters in high-altitude ice clouds: Results of the remote sensing method, *J. Appl. Meteorol*., *36*, 633–648, 1997.

Matrosov, S. Y., Retrievals of vertical profiles of ice cloud microphysics from radar and IR measurements using tuned regressions between reflectivity and cloud parameters, *J. Geophys. Res*., *104*, 16,741–16,753, 1999.

Matrosov, S. Y., T. Uttal, J. B. Snider, and R. A. Kropfli, Estimation of ice cloud parameters from ground-based infrared radiometer and radar measurements, *J. Geophys. Res*., *97*, 11,567–11,574, 1992.

Matrosov, S. Y., B. W. Orr, R. A. Kropfli, and J. B. Snider, Retrievals of vertical profiles of cirrus cloud microphysical parameters from Doppler radar and infrared radiometer measurements, *J. Appl. Meteorol*., *33*, 617–626, 1994.

Matrosov, S. Y., A. J. Heymsfield, J. M. Intrieri, B. W. Orr, and J. B. Snider, Ground-based remote sensing of cloud particle sizes during the 26 November 1991 FIRE-II cirrus case: Comparisons with in situ data, *J. Atmos. Sci*., *52*, 4128–4142, 1995.

Matrosov, S. Y., A. J. Heymsfield, R. A. Kropfli, B. E. Martner, R. F. Reinking, J. B. Snider, P. Piironen, and E. W. Eloranta, Comparisons of ice cloud parameters obtained by combined remote sensor retrievals and direct methods, *J. Atmos. Oceanic Technol*., *15*, 184–196, 1998.

Minnis, P., D. R. Doelling, V. Chakrapani, D. A. Spangenberg, L. Nguyen, R. Palikonda, T. Uttal, R. F. Arduini, and M. Shupe, Cloud coverage and height during FIRE ACE derived from AVHRR data, *J. Geophys. Res*., this issue.

Moran, K. P., B. E. Martner, M. J. Post, R. A. Kropfli, D. C. Welsh, and K. B. Widener, An unattended cloud-profiling radar for use in climate research, *Bull. Am. Meteorol. Soc*., *79*, 443–455, 1998.

Perovich, D. K., et al., Year on ice gives climate insights, *Eos Trans. AGU*, *80*, 481 and 485–486, 1999.

Revercomb, H., F. A. Best, R. G. Dedecker, R. P. Dirkx, R. A. Herbsleb, R. O. Knuteson, J. F. Short, and W. L. Smith, Atmospheric Emitted Radiance Interferometer (AERI) for ARM (Preprints), in *Fourth Symposium on Global Change Studies*, pp. 46–49, Am. Meteorol. Soc., Boston, Mass., 1993.

Rossow, W. B., A. W. Walker, and L. C. Garder, Comparison of ISCCP and other cloud amounts, *J. Clim*., *6*, 2394–2418, 1993.

Sassen, K., Ice cloud content from radar reflectivity, *J. Clim. Appl. Meteorol*., *26*, 1050–1053, 1987.

Sassen, K., and L. Liao, Estimation of cloud content by W-band radar, *J. Appl. Meteorol*., *35*, 2705–2706, 1996.

Sassen, K., G. G. Mace, Z. Wang, M. R. Poellot, S. M. Sekelsky, and R. E. McIntosh, Continental stratus clouds: A case study using coordinated remote sensing and aircraft measurements, *J. Atmos. Sci*., *56*, 2345–2358, 1999.

Stephens, G. L., S.-C. Tsay, P. W. Stackhouse Jr. and P. J. Flatau, The relevance of the microphysical and radiative properties of cirrus clouds to climate and climatic feedback, *J. Atmos. Sci*., *47*, 1742–1753, 1990.

A. S. Frisch, S. Y. Matrosov, M. D. Shupe (corresponding author), and T. Uttal, DSRC, R/ETL6, 325 Broadway, Boulder, CO 80303. (mshupe@etl.noaa.gov)

(Received December 21, 1999; revised July 18, 2000;
accepted July 25, 2000.)